Oncogene (2015), 1–9

www.nature.com/onc

ORIGINAL ARTICLE

A long non-coding RNA links calreticulin-mediated immunogenic cell removal to RB1 transcription

A-S Musahl[1], X Huang[2,3,4], S Rusakiewicz[5,6], E Ntini[1], A Marsico[7,8,9], G Kroemer[2,3,4,10,11], O Kepp[2,3,4] and UA Ørom[1]

A subset of promoters bidirectionally expresses long non-coding RNAs (ncRNAs) of unknown function and protein-coding genes (PCGs) in parallel. Here, we define a set of 1107 highly conserved human bidirectional promoters that mediate the linked expression of long ncRNAs and PCGs. Depletion of the long ncRNA expressed from the RB1 promoter, ncRNA-RB1, reveals regulatory effects different from the RB1-controlled transcriptional program. ncRNA-RB1 positively regulates the expression of calreticulin (CALR) that in response to certain therapeutic interventions can translocate from the endoplasmic reticulum to the cell surface, hence activating anticancer immune responses. Knockdown of ncRNA-RB1 in tumor cells reduced expression of CALR, impaired the translocation of the protein to the cell surface upon treatment with anthracylines and consequently inhibited the cellular uptake by macrophages. In conclusion, co-transcription of ncRNA-RB1 and RB1 provides a positive link between the expression of the two tumor suppressors RB1 and the immune-relevant CALR protein. This regulatory interplay exemplifies disease-relevant co-regulation of two distinct gene products, in which loss of expression of one oncosuppressor protein entails the abolition of additional tumor-inhibitory mechanisms.

Oncogene advance online publication, 12 January 2015; doi:10.1038/onc.2014.424

INTRODUCTION

Several thousand long non-coding RNAs (ncRNAs), that is, functional RNA transcripts not encoding proteins,[1] are encoded in the human genome.[2,3] These transcripts generally display low expression levels and high degrees of tissue specificity, suggesting catalytic roles in the regulation of gene expression. Long ncRNAs reportedly act on various levels of gene regulation mediating either activation or repression of target genes while interacting with a wide range of proteins.[4–8] Initially, long ncRNAs have been found to be involved in the recruitment of histone-modifying complexes to chromatin, which has recently been expanded by reports on the interaction of long ncRNAs with transcription factors and their importance during the formation of co-activator complexes.[7–9]

Research has mostly been focused on the functional characterization of long ncRNAs originating from genomic regions that do not overlap with protein-coding genes (PCGs) and hence those transcripts that are expressed from independent promoters.[5,6,10,11] Although many genome-wide studies in a wide range of organisms established that most PCG promoters are characterized by divergent non-coding transcription, the functional role of those promoter-associated long ncRNAs remains elusive.[12–16] In many cases, antisense transcripts upstream of promoters are unstable and their emergence might be explained by aberrant transcription initiation of RNA polymerase II due to the depletion of nucleosomes on active promoters.[14,17–20] In evolutionary terms, divergent transcription initiation could fuel the emergence of new functional genes, by exposing the transcribed DNA strand to mutagenic alterations as has been reported for the acquisition of splice sites.[21]

Several studies have addressed the regulation of bidirectional transcription,[13,16,18,19,22–27] with three of these shedding light on the functionality of ncRNAs that are bidirectionally expressed from human PCG promoters: Hung *et al.*[28] investigated human cell cycle-regulated genes and identified 58 functional long ncRNAs that are co-expressed with PCGs from bidirectional promoters. One of these transcripts, PANDA (P21 associated ncRNA DNA damage activated), is induced by DNA damage at the CDKN1A promoter and mediates regulation of pro-apoptotic genes.[28] In another study, human embryonic stem cells have been shown to robustly express more than 2000 long ncRNAs bidirectionally from within 2 kb of the transcription start sites (TSS) of PCGs.[16] Transcriptional activation of specific PCGs via the induction of cellular differentiation is coordinated with expression of paired long ncRNAs, suggesting similar functional roles for bidirectionally expressed genes.[16] Furthermore, the long ncRNA Fendrr that seems to be bidirectionally expressed from the Foxf1 promoter in mouse and partly co-expressed with the Foxf1 transcript has been shown to contribute to heart and body wall formation.[29] The co-expression of two genes from a bidirectional promoter suggests a mutual regulation mediated by a shared upstream transcriptional network, and implies that their functions might contribute to the same cellular response independently.

Cancer cells expose proteins at their cell surface, which differ from those of normal cells thereby serving as tumor antigens or activating signals for immune cells.[30,31] One of the recently discovered 'eat-me' signals that are exposed on the cellular

[1]Noncoding RNA Research Group, Max Planck Institute for Molecular Genetics, Berlin, Germany; [2]Team11, Equipe labellisée Ligue contre le Cancer, INSERM U1138, Cordeliers Research Cancer, Paris, France; [3]Université Paris Descartes, Sorbonne Paris Cité, Paris, France; [4]Cell Biology and Metabolomics Platforms, Gustave Roussy Comprehensive Cancer Center, Villejuif, France; [5]Gustave Roussy, Villejuif, France; [6]INSERM, U1015; CICBT507, Villejuif, France; [7]Department of Computational Biology, Max Planck Institute for Molecular Genetics, Berlin, Germany; [8]RNA Bioinformatics group, Max Planck Institute for Molecular Genetics, Berlin, Germany; [9]Free University of Berlin, Berlin, Germany; [10]Université Pierre et Marie Curie, Paris, France and [11]Pôle de Biologie, Hôpital Européen Georges Pompidou, AP-HP, Paris, France. Correspondence: Dr UA Orom, Otto Warburg Laboratories, Max Planck Institute for Molecular Genetics, Ihnestrasse 63, Berlin 14195, Germany.
E-mail: Oerom@molgen.mpg.de
Received 22 August 2014; revised 7 October 2014; accepted 18 November 2014

surface during instances of immunogenic cell death (ICD) is calreticulin (CALR). CALR is an endoplasmic reticulum sessile chaperone that in response to certain chemotherapeutic agents such as anthracyclines or oxaliplatin, translocates to the cellular surface in a pre-apoptotic manner.[32] Surface-exposed CALR then serves as a *de novo* uptake signal to phagocytic cells of the immune system. Thus, ICD can enable the eradication of chemotherapy-resistant cancer cells.

In this study, we used the GENCODE V19 annotation of the human genome to define a set of 1107 highly conserved bidirectional promoters driving the expression of long ncRNAs and PCGs. Most identified promoters are between 100 and 200 bp in length, indicating their potential of bidirectional transcription initiation, emphasizing the possibility of bidirectional expression driven by the same set of transcription factors. For a subset of these promoters we showed their potential to initiate bidirectional transcription. Furthermore, we addressed the function of ncRNA-RB1, a long ncRNA expressed from the RB1 promoter. Separate depletion of ncRNA-RB1 and RB1 mRNA demonstrated that the regulatory programs downstream of both genes contribute to tumor suppressor activity.

RESULTS

To investigate the relationship between divergently encoded long ncRNAs and PCGs in the human genome, we used the GENCODE V19 annotation.[3] We determined the distance between the TSSs of each annotated long ncRNA and its closest PCG encoded on the opposite DNA strand (Figures 1a and b).[33] Within a region of 2 kb around the TSSs of PCG promoters, a promoter size that has previously been used to define PCG-associated long ncRNAs, we found 3891 long ncRNA/PCG pairs.[16] This set of long ncRNA/PCG pairs exhibits a major enrichment of promoters between 100 and 200 bp in length separating the TSSs (Supplementary Figure 1), which is in accordance with previous studies and supports the idea that most long ncRNAs in our data set share a promoter with their associated PCG rather than both genes being expressed from distinct promoters.[34]

When filtering for bidirectional promoters of up to 500 bp in length, the set was narrowed down to nearly half (~45%) of the initial PCG-associated long ncRNAs. After removing overlapping genes, we recovered a final set of 1107 bidirectional ncRNA/PCG pairs (Figures 1a–c, Supplementary Table 1).

Several cancer-related proteins are expressed from bidirectional ncRNA/PCG promoters, for example, the tumor suppressor retinoblastoma 1 (RB1),[35] Nuclear factor NF-kappa-B p100 subunit,[36] glycogen synthase kinase-3 beta[37] and Phosphatidylinositol 4,5-bisphosphate 3-kinase[38] (Supplementary Table 2). Consistently, previous analyses of bidirectional PCG/PCG pairs have shown that DNA-repair genes and genes implicated in somatic cancer are frequently expressed from bidirectional promoters, suggesting that such co-regulation is functionally important.[34,39]

Analysis of conservation of the candidate bidirectional ncRNA/PCG promoters showed significantly higher conservation rates of bidirectional ncRNA/PCG promoters as compared with the average PCG promoter ($P = 6.5 \times 10^{-5}$; Figure 1d), implying an evolutionary conservation of the genomic head-to-head arrangement of the 1107 candidate ncRNA/PCG pairs. This supports the notion that co-regulation of both paired genes is physiologically relevant.

To determine the potential of defined promoters to initiate bidirectional transcription, we tested four candidates (driving the expression of *CCNG1*, *FKTN*, *MAGOH* and *RB1* genes) in a reporter assay. For the reporter assay the promoters were inserted into a vector containing firefly and *Renilla reniformis* luciferase genes in a head-to-head orientation to simultaneously measure the expression of both reporter genes (Figure 2a). For all candidates, orientation of the promoter was directed so that firefly luciferase activity represents the promoter strength in the PCG direction and *Renilla reniformis* luciferase activity represents the promoter strength relevant to the long ncRNA expression. All tested promoters mediated high firefly luciferase activity, indicating their potential to initiate transcription of paired ncRNAs and PCGs (Figure 2b). Importantly, the four candidate bidirectional promoters more efficiently expressed *Renilla reniformis* luciferase than do two control promoters that appear predominantly unidirectional (GAPDH and TK; Figure 2b). To determine the significance of this observation, we calculated the ratio between firefly and *Renilla reniformis* luciferase activities for all tested promoters. A value close to 1 implied a high bidirectional potential of a promoter, whereas potential unidirectional promoters were characterized by

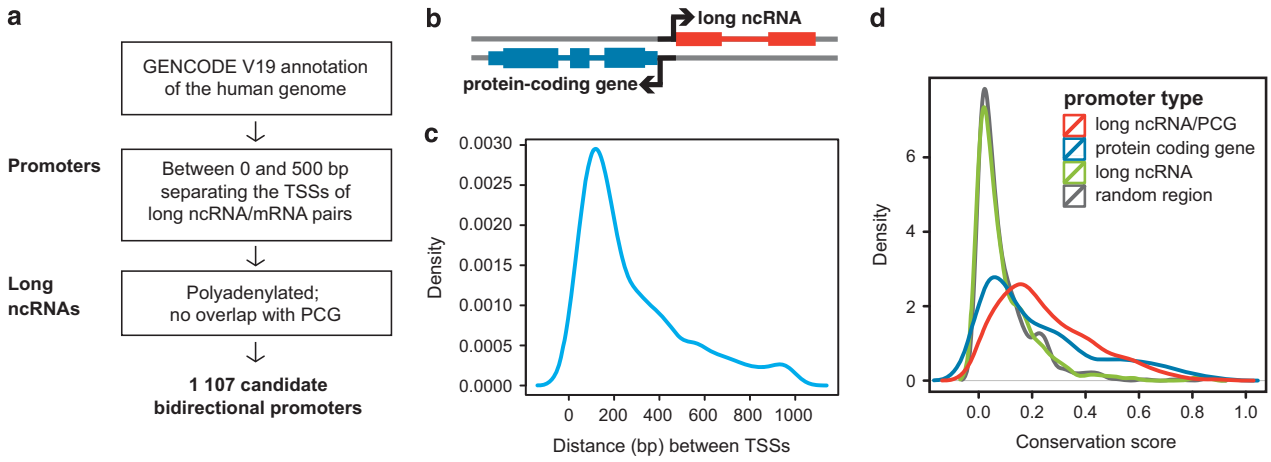

Figure 1. Transcription of long ncRNAs and PCGs from bidirectional promoters. (**a**) Criteria for promoters and long ncRNAs to define 1107 candidate bidirectional promoters of long ncRNA/PCG pairs in the human genome. (**b**) Schematic of genomic arrangement of defined long ncRNA/PCG pairs (orange and blue, respectively), which are listed in Supplementary Table 1. (**c**) Density plot showing the distribution of distances between TSSs of divergently encoded long ncRNA/PCG pairs (1 kb window), for those long ncRNAs not overlapping a PCG throughout their genomic region. (**d**) Density plot showing the distribution of conservation scores for promoters of bidirectional ncRNA/PCG pairs, PCG, long ncRNAs and random regions. Bidirectional ncRNA/PCG promoters exhibit significantly higher conservation rates than the average PCG promoters ($P = 6.5 \times 10^{-5}$).

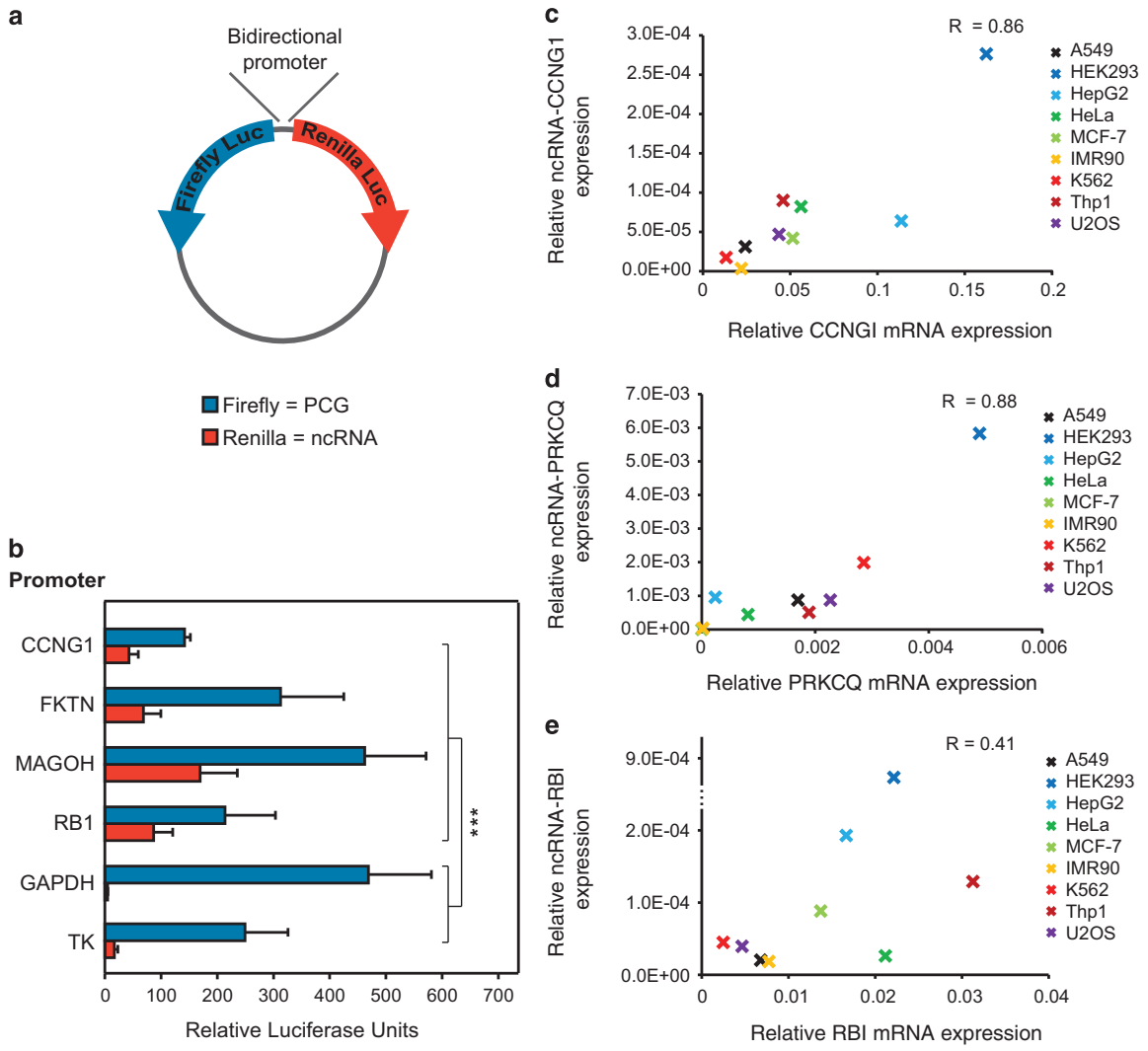

Figure 2. ncRNA/PCG expression from bidirectional promoters. (**a**) Schematic of the reporter vector to determine bidirectional promoter activity. Promoters are inserted so that Firefly luciferase activity represents the promoter strength in the PCG direction and *Renilla* luciferase activity represents the promoter strength in the ncRNA direction. (**b**) Bidirectional promoter activities of CCNG1, FKTN, MAGOH and RB1 candidate bidirectional promoters and GAPDH and TK as control promoters are represented by the relative luciferase units for both Firefly and *Renilla* luciferases. Mean values ± s.d. are shown, $n \geqslant 3$ replicates. ***$P < 0.005$. (**c**–**e**) Relative expression levels of paired transcripts. (**c**) CCNG1, (**d**) PRKCQ and (**e**) RB1 promoters as determined by qRT–PCR. The *y* axis represents ncRNA expression level and the *x*-axis represents mRNA expression level for nine cell lines (A549, HEK293, HeLa, HepG2, IMR90, K562, MCF7, Thp1 and U2OS). Expression values are presented relative to the value of Actin as reference gene. Mean values ± s.d. are shown, $n \geqslant 3$ replicates.

low values (CCNG1 = 0.30, FKTN = 0.22, MAGOH = 0.38, RB1 = 0.43, GAPDH = 0.01 and TK = 0.07). Importantly, the values for candidate bidirectional promoters were significantly higher than for control promoters ($P \leqslant 0.001$).

Next, we determined relative transcript levels of three ncRNA/PCG pairs across nine cell lines using quantitative reverse transcriptase (qRT)–PCR. For the CCNG1, PRKCQ and RB1 promoters, both transcripts were detectable in each of the cell lines examined. Expression levels for ncRNAs and respective mRNAs differed in several orders of magnitude and showed various degrees of correlation, as determined by calculating Pearson correlation coefficients ($R_{CCNG1} = 0.86$, $R_{PRKCQ} = 0.88$, $R_{RB1} = 0.41$ (Figures 2c–e). A high correlation between endogenous ncRNA and PCG expression was observed for the CCNG1 and PRKCQ promoters, whereas the correlation for RB1 was less pronounced, potentially due to additional regulation of transcription and transcript stability.

Among the candidate promoters, the one driving expression of RB1 has been intensively studied. Within the RB1 promoter sequence, binding sites of at least five transcription factors that are responsible for regulated expression of the *RB1* gene have been identified: ATF,[40] p53,[41] E2F1,[42] E4TF1[43] and Sp1[40] (Figure 3a). ATF, SP1 and E4TF1 are activators of the *RB1* gene,[40,44,45] and p53 and E2F1 (in complex with pRB1 itself) act as repressors.[41,46] The TSSs of RB1 and ncRNA-RB1 are separated by a GC-rich 114-bp-long promoter region. As it is often observed in metazoan GC-rich promoters, the ncRNA-RB1/RB1 promoter lacks a TATA box,[47] further supporting the bidirectional nature of the region. Studies of the RB1 promoter have described that deletion of a 17-bp region overlapping the binding sites of SP1, ATF and E2F1 completely abrogates promoter activity in the RB1 direction.[44] We observed that this deletion not only reduces the promoter activity in the RB1 direction, but also decreased that in the ncRNA-RB1 direction, when introduced into the bidirectional luciferase vector (Figure 3b). We further showed the co-regulation

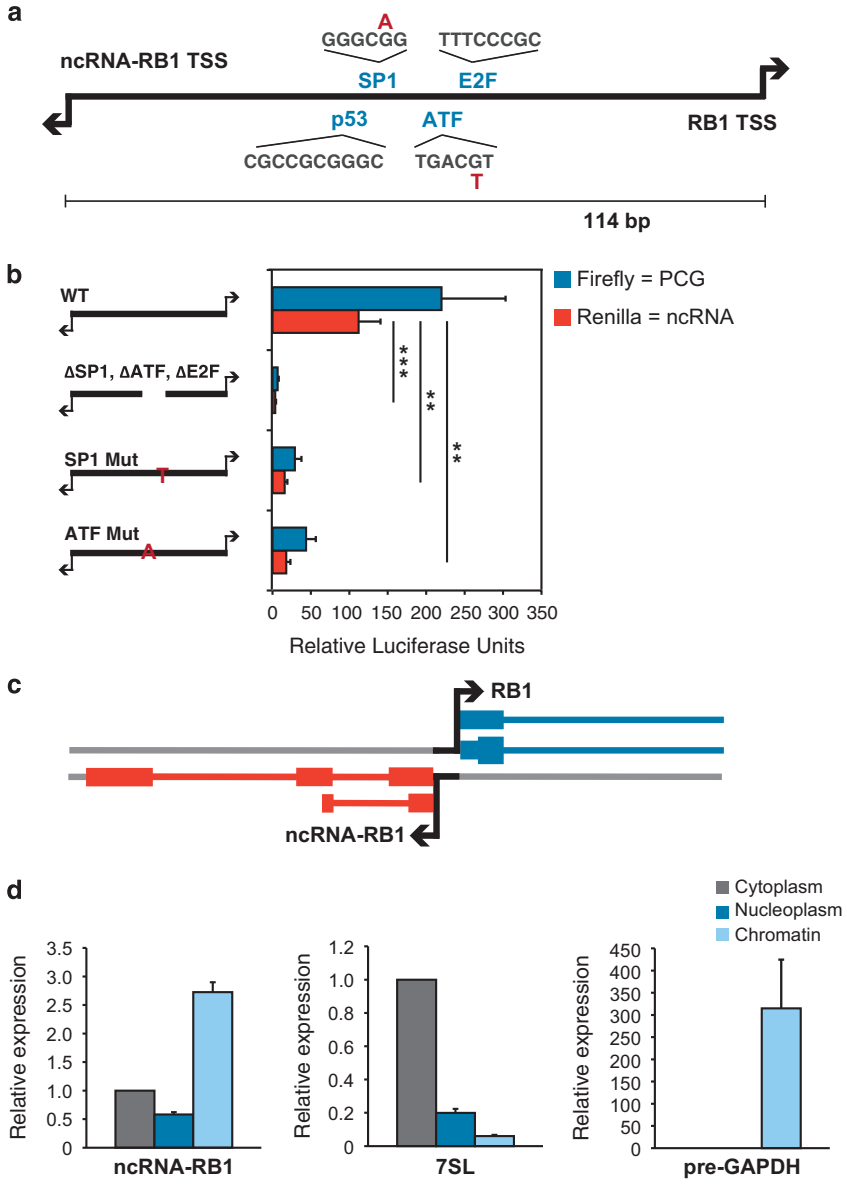

Figure 3. The ncRNA-RB1/RB1 promoter and genomic locus. (**a**) Schematic of the ncRNA-RB1 promoter. ncRNA-RB1 and RB1 TSSs are separated by a 114-nucleotide promoter region that encodes the binding sites of ATF, E2F, p53 and SP1 transcription factors. Two retinoblastoma-associated point mutations in the ATF (G → T, red) and SP1 binding sites (G → A, red) are shown. (**b**) Bidirectional RB1 promoter activities of the wild-type promoter (WT), the promoter with deleted SP1, ATF and E2F binding sites (ΔSP1, ΔATF and ΔE2F), the RB1 promoter with mutated SP1-binding site (SP1 Mut) and the RB1 promoter with mutated ATF-binding site (ATF Mut) are represented by relative luciferase units for both Firefly and *Renilla* luciferases. The mean values ± s.d. are shown, $n \geqslant 3$ replicates. $^{**}P < 0.01$, $^{***}P < 0.005$. (**c**) Schematic of the ncRNA-RB1 genomic locus in the human genome. Two splice forms of ncRNA-RB1 are annotated in the GENCODE V19 annotation (depicted in dark orange). (**d**) Localization of transcripts in cellular fractions from A549 cells. The relative expression of ncRNA-RB1 within the cellular fractions was determined by qRT–PCR. Relative expressions of 7SL and pre-GAPDH transcripts were determined as control for the purity of cellular fractions. The mean values ± s.d. are shown, $n = 3$ replicates.

of transcription initiation by the RB1 promoter by introducing two distinct retinoblastoma-associated mutations into the Luciferase reporter, that are located within the ATF and SP1 transcription factor-binding sites.[40] Both point mutations dramatically reduced the bidirectional RB1 promoter activity, potentially also contributing to ncRNA-RB1 expression *in vivo* (Figure 3b).

ncRNA-RB1 is encoded by a 7.1-kb region 114 bp upstream of the *RB1* gene. The transcript is annotated to consist of two isoforms with a maximum size of 1.14 kb (Figure 3c). We determined the subcellular distribution of ncRNA-RB1 transcript levels by cellular fractionation of A549 cells followed by RNA isolation and qRT–PCR. This shows a predominantly nuclear localization of ncRNA-RB1 (Figure 3d).

To gain insight into the regulatory functions of ncRNA-RB1 and to infer the involvement of this ncRNA within regulatory circuits of RB1, we individually depleted both transcripts from A549 cells using small interfering RNAs (siRNAs). Knockdown of both transcripts was efficient, yielding a 60–80 percent decrease of transcript levels (Figures 4a and d). Furthermore, reduction in RB1 protein levels following knockdown of RB1 mRNA was confirmed by western blot analysis (Figure 4e). When depleting ncRNA-RB1 no effects on RB1 transcript or protein levels were observed (Figures 4a, b and e). Likewise, depletion of RB1 mRNA did not affect the expression of ncRNA-RB1 (Figures 4c and d) suggesting that the two transcripts do not regulate each other but rather contribute to independent regulatory functions.

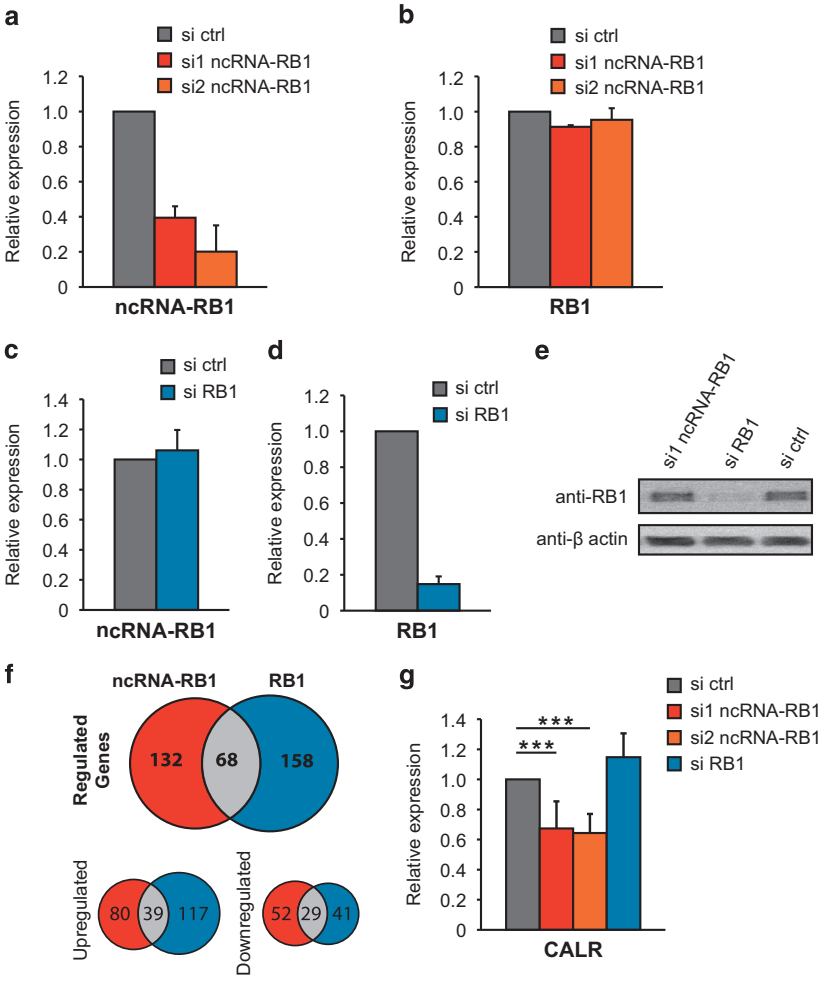

Figure 4. ncRNA-RB1 and RB1 regulate distinct target genes. (**a**) Knockdown of ncRNA-RB1 in A549 cells using two different siRNAs against ncRNA-RB1. As control, A549 cells were transfected with a non-targeting control siRNA. (**b**) Determination of RB1 expression levels following knockdown of ncRNA-RB1 using two siRNAs. (**c**) Determination of ncRNA-RB1 expression levels following siRNA-mediated knockdown of RB1 mRNA. (**d**) Knockdown of RB1 mRNA in A549 cells using one siRNA. As control, A549 cells were transfected with a nontargeting control siRNA. (**e**) Western blot analysis to determine RB1 protein levels following siRNA-mediated knockdown of RB1 mRNA and of ncRNA-RB1 in A549 cells. β-actin protein levels are depicted as loading control. (**f**) Venn diagram depicting the number of regulated genes upon knockdown of ncRNA-RB1 (red) and RB1 (blue) determined as described in Materials and methods. Upper diagram shows the total number of regulated genes for each knockdown. The genes commonly regulated by ncRNA-RB1 and RB1 are depicted in gray. Lower diagrams show number of up- and downregulated genes. (**g**) Determination of relative expression levels of the ncRNA-RB1 target gene CALR following knockdown of ncRNA-RB1 and knockdown of RB1 mRNA. Expression levels are presented relative to the value of Actin as reference gene as determined by qRT–PCR. The mean values ± s.d. are shown, $n \geqslant 3$ replicates. ***$P < 0.005$.

In order to identify targets of ncRNA-RB1 we performed RNA-sequencing of poly(A)-enriched RNA from A549 cells after treatment with siRNAs against ncRNA-RB1. Cells depleted of RB1 were used for comparison of gene expression differences following knockdown of the two transcripts. The knockdown of ncRNA-RB1 resulted in differential expression of 200 genes that are not significantly enriched in any particular GO term (Figure 4f and Supplementary Table 3). The most highly regulated transcript in terms of absolute change in RPKM encodes the protein CALR (Figure 4g), an endoplasmic reticulum-sessile chaperone that has been shown to be important for ICD by serving as an 'eat-me' signal presented by apoptotic cells.[30,32] To further study the regulation of CALR by ncRNA-RB1, we monitored CALR protein levels following knockdown of ncRNA-RB1. Western blot analysis revealed a more than 80 percent reduction of CALR protein levels 48 h after siRNA-mediated knockdown of ncRNA-RB1, showing that the downregulation of CALR is pronounced also on the protein level (Figure 5a). To determine whether the regulation of CALR by ncRNA-RB1 occurred on the transcriptional level, we subjected control or ncRNA-RB1-depleted cells to subcellular fractionation, and determined the abundance of CALR mRNA in chromatin-associated fractions (Figure 5b). A significant decrease in CALR mRNA levels was observed in the chromatin fraction, suggesting a role of transcriptional regulation of CALR expression by ncRNA-RB1 (Figure 5b). Decreased levels of ncRNA-RB1 were observable, although not statistically significant in the chromatin fraction, possibly because of the inefficient siRNA-mediated effects on chromatin (Figure 5c). GAPDH levels on chromatin did not show any changes following knockdown of ncRNA-RB1 (Figure 5d). We further determined the subcellular distribution of CALR protein by immunofluorescence staining of control and ncRNA-RB1-depleted U2OS cells (Figure 6a). These results are in accordance with the preponderant localization of CALR protein in the endoplasmic reticulum.[32] CALR reduction on the protein level by more than 60 percent was further quantified by cytofluorometric analysis (Figure 6b).

Next, we addressed the functional impact of ncRNA-RB1 on CALR surface exposure and the potential effect on immunogenic

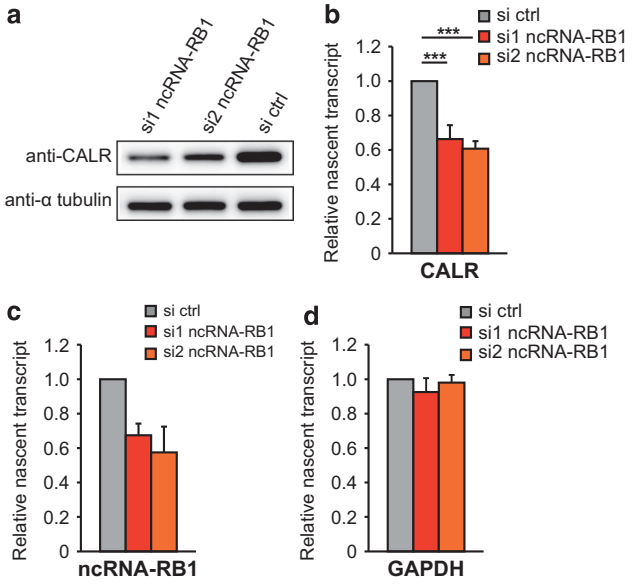

Figure 5. ncRNA-RB1 regulates CALR expression. (**a**) Western blot analysis to determine CALR protein levels following siRNA-mediated knockdown of ncRNA-RB1 in A549 cells. α-tubulin protein levels are depicted as loading control. (**b**) CALR expression levels on chromatin following knockdown of ncRNA-RB1 in A549 cells. (**c**) Knockdown efficiency of ncRNA-RB1 on chromatin in A549 cells. (**d**) GAPDH expression levels on chromatin following knockdown of ncRNA-RB1. The relative expression of ncRNA-RB1, CALR and GAPDH within the cellular fractions was determined by qRT–PCR. The mean values ± s.d. are shown, $n = 3$ replicates. $^{***}P < 0.005$.

cell removal. We therefore treated ncRNA-RB1-depleted U2OS cells with mitoxantrone (MTX), a chemotherapeutic agent that induces cell surface translocation of CALR.[32,48] CALR exposed at the cell membrane (ecto-CALR) was monitored by cell surface immunofluorescence staining of live cells followed by cytofluorometry. Ecto-CALR levels were strongly reduced upon depletion of ncRNA-RB1 as compared with control cells (Figures 6c and d). As cell surface exposure of CALR is a major stimulus of phagocytosis, we hypothesized that a substantial decrease in ecto-CALR protein levels would interfere with a subsequent uptake by immune cells. Accordingly, as compared with controls, ncRNA-RB1 depletion resulted in reduced uptake of MTX-treated cells by human macrophages in an *in vitro* phagocytosis assay (Figures 6e and f).

DISCUSSION

The functions of long ncRNAs that are associated with the promoters of PCGs remain mostly unclear, although this class of transcripts is increasingly detected in many genome-wide studies focusing on eukaryotic promoters.[12,13,16,22,23] Previous studies have proposed a role for PCG-associated antisense long ncRNAs in the direct regulation of their protein partner, for example, by interaction with the protein-coding DNA region or their complementary mRNA.[49,50] In contrast to these findings, the RB1 promoter-associated long ncRNA-RB1 described in this study does not regulate the transcription of RB1. ncRNA-RB1 seems to mediate tumor-inhibitory mechanisms through the regulation of its target genes. The idea that co-transcription could entail co-functionality of paired gene products is supported by the observation that divergent PCG/PCG pairs in the human genome (around 10% of all PCGs) are enriched in specific functional categories, such as DNA repair and the regulation of cell cycle and metabolism.[51]

As the annotated promoter region separating the TSSs of ncRNA-RB1 and RB1 is only 114 bp in size, we reasoned that the transcripts are likely to be co-expressed from a shared bidirectional promoter. Conceptually, the transcript pairs originating from relatively short bidirectional promoters should be regulated in a coordinated manner, as on nucleosome-free promoters the establishment of an active transcription environment on one TSS facilitates transcription initiation by polymerase II also at the divergent TSS.[20] The experimental validation of bidirectional promoter activity demonstrated the ability of the promoters to initiate transcription in both directions. Reduced bidirectional promoter activity upon introduction of single base pair mutations argues for a regulation by the same transcription factors and linked expression of the two transcripts. The high conservation rate we observed for the set of bidirectional ncRNA/PCG promoters further supports the importance of preservation of regulatory elements such as transcription factor-binding sites. The simultaneous transcription of long ncRNA/PCG pairs might be mediated by shared binding sites within the promoter region. Whereas the reporter assays for four candidate bidirectional promoters showed similar capabilities to mediate transcription in both directions, *in vivo* expression analysis for some of these endogenous promoters by qPCR showed a 100-fold difference between expression levels of long ncRNAs and PCGs for most cases. This suggests that further regulatory mechanisms are involved, affecting transcriptional elongation or post-transcriptional stability of both RNAs, which could also explain the low correlation in expression for some of the paired transcripts. The exosome has been suggested to be involved in the regulation of promoter-associated transcripts.[14] However, our attempts to demonstrate exosome involvement for selected long ncRNAs did not yield statistical significant differences.

The ncRNA-RB1 target gene *CALR* displayed the most pronounced differential expression in terms of absolute change in RPKM upon ncRNA-RB1 knockdown. The significance of this observation becomes clear when considering the high cellular abundance of this endoplasmic reticulum-sessile protein and its function as a major Ca^{2+}-binding protein and chaperone. The CALR protein has been shown to serve as an 'eat-me' signal for immune cells when exposed to the plasma membrane.[30,32,48,52] The transcriptional regulation of CALR by ncRNA-RB1 extended to the surface translocation of CALR observed upon MTX treatment. Whereas surface CALR was not directly affected by the knockdown of ncRNA-RB1, the translocation upon MTX treatment was markedly reduced. This difference in translocation was reflected in the reduced uptake of cancer cells by human macrophages, and thus assigns an important role to ncRNA-RB1 in the regulation of immunogenic cell removal. It has been proposed recently that tumorigenic cells are not only involved in disabling cell-intrinsic death programs (such as apoptosis) but they must also avoid programmed cell removal by phagocytes, a process that is also referred to as 'phagoptosis'.[30] One of the aims of chemotherapy is therefore to elicit an anticancer immune response by inducing the uptake of dying cancer cells by phagocytes.

In conclusion, we showed that ncRNA-RB1 links the transcription regulation of RB1 to expression of CALR and can mediate differential recognition of cancer cells by macrophages in ICD. The possibility that neoplastic cells can simultaneously abrogate expression of RB1 and ncRNA-RB1, caused by, for example, RB1 promoter mutation or hypermethylation, could have significant therapeutic relevance.

MATERIALS AND METHODS

Promoter conservation analysis

The promoter regions of bidirectionally encoded long ncRNAs were defined as 700-bp regions surrounding the annotated TSS of long ncRNAs (500 bp upstream and 200 bp downstream). Promoter regions of long

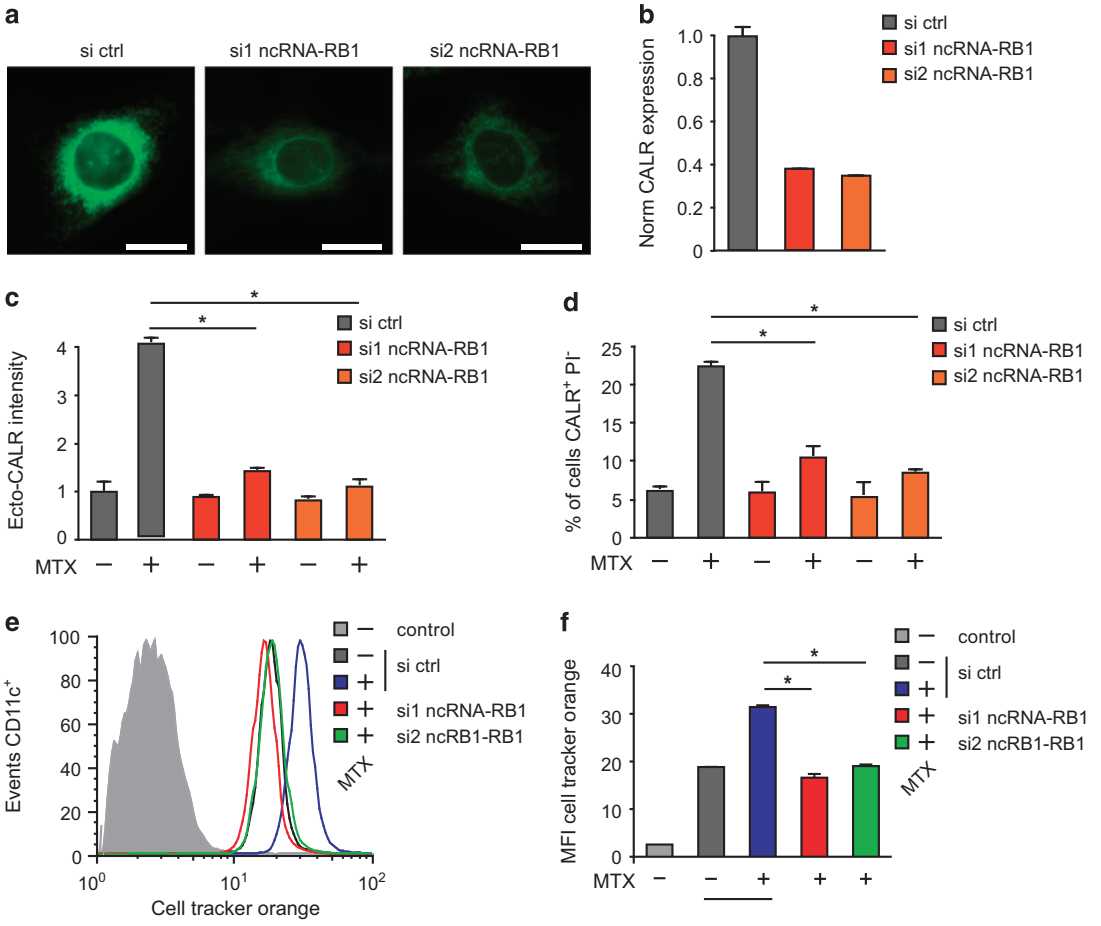

Figure 6. Regulation of programmed cell removal by ncRNA-RB1. (**a**) Representative images of CALR protein expression (green) in U2OS cells treated with siRNAs against ncRNA-RB1 or scrambled control siRNAs obtained by immunohistochemistry. The scale bar equals 10 μm. (**b**) Nine view fields per condition were analyzed by automated image segmentation and the fluorescence intensity of CALR immunostaining was normalized to siRNA controls. (**c**, **d**) U2OS cells treated with siRNAs against ncRNA-RB1 or scrambled control siRNAs were subjected to 2 μM MTX for 12 h and surface-exposed CALR was evaluated by immunohistochemistry and subsequent flow cytometry. Dead cells were excluded by counterstaining with propidium iodide and mean fluorescence intensity as well as the percent of CALR-positive cells were determined. Statistical analysis was conducted between the MTX-treated samples. (**e**, **f**) FITC-labeled macrophages were coincubated for 2 h with celltracker orange stained U2OS cells treated with siRNAs and subjected to 2 μM MTX for 12 h as indicated. The celltracker fluorescence intensity of CD11b-FITC-labeled PBMC was measured as an indicator for tumor cell uptake. Mean values ± s.d. are shown, $n = 3$ replicates. $^*P < 0.05$.

ncRNA genes in general and PCGs were defined in the same way. For comparison, intergenic regions of 700 bp were extracted from random locations in the genome and masked for repetitive regions. Ten promoter sets of comparable size to the 1107 bidirectional promoters were considered for each of the other promoter classes and the results were averaged over 10 data sets. Position-wise conservation scores were computed from the PhastCons vertebrate conservation track from UCSC.[53] An average conservation score was then computed for each of the 700-bp regions, and the distribution of these scores plotted for each class.

Cell culture

HEK293, A549 and U2OS cells were cultured in complete DMEM medium (Gibco/LifeTechnologies, Carlsbad, CA, USA) supplemented with 10% fetal bovine serum (FBS) and penicillin–streptomycin (Gibco) at 37 °C with 5% CO_2.

Cloning of pGL3 reporter plasmids

The *Kpn*I and *Mlu*I sites in the pGL3-Basic vector (Promega, Fitchburg, WI, USA) were used to insert the *Renilla reniformis* luciferase reporter gene amplified from the pRL-TK vector (Promega), yielding a head-to-head orientation of both reporter genes. Promoters were cloned into the *Bgl*II and *Hin*dIII restriction sites.

Primer sequences: Renilla Luciferase (5′-GGACGCGTCACTATAGGCTAG CCACCATGA-3′, 5′-GGGGTACCTGGATCCTTATCGATTTTACCA-3′), CCNG1 promoter (5′-GGAGATCTCAGCCGATTGACCTGACC-3′, 5′-GGAAGCTTGAGAC AACTCGGCCCTGAT-3′), FKTN promoter (5′-GGAGATCTGGTGAGGATGCGAC AAGAGT-3′, 5′-GGAAGCTTGAGCCTCCCGTACCTTACCT-3′), MAGOH promoter (5′-GGAGATCTTGCAGTCTTGTTGCCACTTC-3′, 5′-GGAAGCTTGCCTGAACT TCCAAGAGCAA-3′), RB1 promoter (5′-GGAAGCTTGCAACTGAGCGCCGC GTC-3′, 5′-GGAGATCTAGCGCCCCAGTTCCCCAC-3′). The TK promoter was exerted from the pRL-TK plasmid using *Bgl*II and *Hin*dIII restriction enzymes.

Luciferase assay

HEK293 cells were transfected with Lipofectamine 2000 (LifeTechnologies) in 96-well white plates with 200 ng of the respective plasmids. Twenty-four hours after transfection, luciferase activity was measured using the Dual-Glo Luciferase Assay System (Promega) according to the manufacturer's protocol. Firefly and *Renilla reniformis* luciferase counts for promoters were normalized to their respective counts in the no-promoter vector.

Quantitative real-time PCR

Total RNA was extracted from cells with TRIzol (Life Technologies) following the manufacturer's instructions and treated with DNaseI (New

England Biolabs (NEB), Ipswich, MA, USA). cDNA was synthesized using the High Capacity RNA-to-cDNA Kit (Life Technologies) and qPCR was performed using the Fast SYBR Green Master Mix (Life Technologies) on a 7900HT Fast Real-Time PCR System (Applied Biosystems, Foster City, CA, USA). The relative expression was calculated by normalizing to the Actin expression level as reference control gene.

The sequences of the real-time primers are: ncRNA-CCNG1 (5′-AGT GGTTCTGCCCCATCTTT-3′, 5′-GTGCTTTGAGAGGCCAAAGT-3′), CCNG1 mRNA (5′-TCACCTTCCAACAATTCCTGA-3′, 5′-AAGGTTGTGGAGAAAGGC TTC-3′), ncRNA-PRKCQ (5′-GGTGGGACTGCTTTCAACTT-3′, 5′-GCTGTTATCC GTTTGCCATT-3′), PRKCQ mRNA (5′-TGAGAGGTGCAGGAAGAACA-3′, 5′-GCC TTCCGTCTCAAATTCAT-3′), ncRNA-RB1 (5′-GGACGTGCTTCTACCCAGAAC-3′, 5′-TCCTTCTCAGTTGACGAGTTCA-3′) , RB1 (5′-GAGCAAGGTCTAAGGCAGGA-3′, 5′-CTGGCAGTTTGTTGCTTCAG-3′) and β-actin (5′-CGACAGGATGCAGA AGGAG-3′, 5′-GTACTTGCGCTCAGGAGGAG-3′).

RNA interference

dsiRNA oligos from IDTDNA (si1 ncRNA-RB1: sense 5′-GACGCUAAGUCAUG AGGAAUUAAAC-3′, antisense 5′-GUUUAAUUCCUCAUGACUUAGCGUCCC -3′; si2 ncRNA-RB1: sense 5′-CUGAACUCGUCAACUGAGAAGGAAA-3′, anti-sense 5′-UUUCCUUCUCAGUUGACGAGUUCAGAU-3′; si1 RB1: sense 5′-CUCCCAUGUUGCUCAAAGAACCATA-3′, antisense 5′-UAUGGUUCUUUGA GCAACAUGGGAGGU-3′) were used. As a negative control we used DS NC1 (IDT DNA).

Cells were transfected at a final dsiRNA concentration of 10 nM using Lipofectamine 2000 (Life Technologies) according to the manufacturer's protocol. Cells were collected 24 h post transfection for RNA isolation and 48 h post transfection for western blot analysis.

RNA isolation and sequencing

Total RNA was extracted using TRIzol (Life Technologies) and RNAseq libraries were prepared with the TruSeq RNA Sample Preparation Kit v2. Sequencing was performed on a HiSeq 2000 instrument (Illumina, San Diego, CA, USA) using paired-end sequencing (2×50 bp). Sequencing data were subjected to the quality control (QC) using defined metrics on an automated quality-control pipeline that combines published tools as FastQC (http://www.bioinformatics.babraham.ac.uk/projects/fastqc) with in-house standardized methods. All reads that passed quality metrics were mapped to the latest human genome build (UCSC hg19). Sequencing duplicated reads were removed using PicardTools (http://picard.sourceforge.net/). For alignment the most recent version of Bowtie2[54] and TopHat2[55] were used. Read counting/summarizing was performed using Cufflinks2.[56]

Immunoblotting

Proteins were resolved using NuPAGE 4–12% Bis-Tris gels (Life Technologies) and 1X NuPAGE MOPS SDS Running Buffer (Life Technologies) and transferred onto PVDF membranes. Membranes were probed with a primary antibody (mouse anti-RB1 (4H1, Cell Signaling), mouse anti-CALR (FMC 75, Abcam), mouse anti-β-actin (8H10D10, Cell Signaling), mouse anti-α-tubulin (DM1A, Cell Signaling)).

Cellular fractionation

Cellular fractions for RNA isolation were prepared from $\sim 4 \times 10^6$ cells as described in[57] except for the proteinase K treatment of cytoplasmic and nuclear fractions.

Immunofluorescence

Ten thousand human osteosarcoma U2OS cells seeded in poly-L-lysine-coated 96-well Black/Clear Imaging Plates (BD Biosciences, Franklin Lakes, NJ, USA) were subjected to siRNA-mediated knockdown of ncRNA-RB1 as described above. Forty-eight hours later the cells were fixed with 3.7% paraformaldehyde (Sigma-Aldrich, St Louis, MO, USA) containing hoechst 33342 (Sigma-Aldrich), permeabilized with 0.1% triton-X100 and stained with anti-CALR antibody (Abcam, Cambridge, UK) for 30 min and subsequent Alexafluor-488-conjugated secondary antibody (Invitrogen, Carlsbad, CA, USA) diluted in blocking buffer (2% FBS, v/v in phosphate-buffered saline (PBS)). Nine view fields per well were acquired by means of a Molecular Devices IXM XL automated microscope and images were analyzed for cytoplasmic fluorescence intensity by using the Metaxpress software v. 5.1 (Molecular Devices, Sunnyvale, CA, USA).

Flow cytometry

Cells were collected, washed twice with PBS and thereafter incubated with anti-CALR antibody (Abcam) diluted in cold blocking buffer (2% FBS, v/v in PBS) for 30 min on ice, followed by washing and incubation with AlexaFluor 488-conjugates (Invitrogen) in blocking buffer (for 30 min). Thereafter, cells were washed in cold PBS, PI was added to the final concentration of 1 μg/ml and samples were analyzed by means of a FACScan cytofluorometer (Becton Dickinson, Franklin Lakes, NJ, USA). Isotype-matched IgG antibodies (Cell Signaling Technology, Danvers, USA) were used as negative staining control, and the analysis was limited to living (PI^-) cells. Data were statistically evaluated by means of the Cell Quest Software package (Becton Dickinson).

Macrophage uptake assay

Peripheral blood mononuclear cells (PBMCs) were isolated from freshly harvested blood samples of healthy volunteers by means of Ficoll density gradient centrifugation. Macrophages were purified using a CD11b-positive selection (Miltenyi, Bergisch Gladbach, Germany) and labeled with CD11b-FITC antibody (Miltenyi) following the manufacturer's protocol. Fluorescein isothiocyanate (FITC)-labeled macrophages were incubated for 2 h at 37 °C with orange cell tracker (Life technology)-stained U20S human osteosarcoma cells, that were subjected to siRNA-mediated knockdown of ncRNA-RB1 as described above and subsequently treated with 2 μM mitoxantrone for additional 12 h to induce CALR surface exposure. Cells were recovered and stained with the viability marker 4,6-diamidino-2-phenylindole (Sigma) and immediately acquired on a Cyan ADP flow cytometer (Beckman Coulter, Brea, CA, USA). The uptake of apoptotic tumor cells stained with cell tracker orange by CD11b-FITC-positive macrophages was analyzed using the FlowJo software (Tree Star, Ashland, OR, USA).

Statistics

Experiments were carried out in minimally three independent replicates. Statistical analyses were performed using two-tailed Student's *t*-test.

CONFLICT OF INTEREST

The authors declare no conflict of interest.

ACKNOWLEDGEMENTS

Work in the laboratories of GK and OK are suppported by the Ligue contre le Cancer (équipe labelisée); Agence National de la Recherche (ANR); Association pour la recherche sur le cancer (ARC); Cancéropôle Ile-de-France; AXA Chair for Longevity Research; Institut National du Cancer (INCa); Fondation Bettencourt-Schueller; Fondation de France; Fondation pour la Recherche Médicale (FRM); the European Commission (ArtForce); the European Research Council (ERC); the LabEx Immuno-Oncology; the SIRIC Stratified Oncology Cell DNA Repair and Tumor Immune Elimination (SOCRATE); the SIRIC Cancer Research and Personalized Medicine (CARPEM); and the Paris Alliance of Cancer Research Institutes (PACRI). Work in the laboratory of UAØ is supported by the German Ministry of education and research through the Alexander von Humboldt Foundation Sofja Kovalevskaja Award.

AUTHOR CONTRIBUTIONS

A-SM conceived the experiments, performed all experiments except those in Figure 6 and interpreted the data. XH and SR performed the experiments in Figure 6. EN and AM performed bioinformatic analysis. GK and OK conceived the experiments in Figure 6, supervised research and interpreted data. UAØ conceived the experiments, supervised research and interpreted data. A-SM, GK, OK and UAØ wrote the manuscript. All authors read and approved the manuscript.

REFERENCES

1 Orom UA, Shiekhattar R. Long noncoding RNAs usher in a new era in the biology of enhancers. *Cell* 2013; **154**: 1190–1193.
2 Cabili MN, Trapnell C, Goff L, Koziol M, Tazon-Vega B, Regev A *et al.* Integrative annotation of human large intergenic noncoding RNAs reveals global properties and specific subclasses. *Genes Dev* 2011; **25**: 1915–1927.

3 Derrien T, Johnson R, Bussotti G, Tanzer A, Djebali S, Tilgner H *et al.* The GENCODE v7 catalog of human long noncoding RNAs: analysis of their gene structure, evolution, and expression. *Genome Res* 2012; **22**: 1775–1789.
4 Zhao J, Sun BK, Erwin JA, Song JJ, Lee JT. Polycomb proteins targeted by a short repeat RNA to the mouse X chromosome. *Science* 2008; **322**: 750–756.
5 Rinn JL, Kertesz M, Wang JK, Squazzo SL, Xu X, Brugmann SA *et al.* Functional demarcation of active and silent chromatin domains in human HOX loci by noncoding RNAs. *Cell* 2007; **129**: 1311–1323.
6 Wang KC, Yang YW, Liu B, Sanyal A, Corces-Zimmerman R, Chen Y *et al.* A long noncoding RNA maintains active chromatin to coordinate homeotic gene expression. *Nature* 2011; **472**: 120–124.
7 Lai F, Orom UA, Cesaroni M, Beringer M, Taatjes DJ, Blobel GA *et al.* Activating RNAs associate with Mediator to enhance chromatin architecture and transcription. *Nature* 2013; **494**: 497–501.
8 Melo CA, Drost J, Wijchers PJ, van de Werken H, de Wit E, Oude Vrielink JA *et al.* eRNAs are required for p53-dependent enhancer activity and gene transcription. *Mol Cell* 2013; **49**: 524–535.
9 Trimarchi T, Bilal E, Ntziachristos P, Fabbri G, Dalla-Favera R, Tsirigos A *et al.* Genome-wide mapping and characterization of notch-regulated long noncoding RNAs in acute leukemia. *Cell* 2014; **158**: 593–606.
10 Orom UA, Derrien T, Beringer M, Gumireddy K, Gardini A, Bussotti G *et al.* Long noncoding RNAs with enhancer-like function in human cells. *Cell* 2010; **143**: 46–58.
11 Guttman M, Amit I, Garber M, French C, Lin MF, Feldser D *et al.* Chromatin signature reveals over a thousand highly conserved large non-coding RNAs in mammals. *Nature* 2009; **458**: 223–227.
12 Core LJ, Waterfall JJ, Lis JT. Nascent RNA sequencing reveals widespread pausing and divergent initiation at human promoters. *Science* 2008; **322**: 1845–1848.
13 Neil H, Malabat C, d'Aubenton-Carafa Y, Xu Z, Steinmetz LM, Jacquier A. Widespread bidirectional promoters are the major source of cryptic transcripts in yeast. *Nature* 2009; **457**: 1038–1042.
14 Preker P, Nielsen J, Kammler S, Lykke-Andersen S, Christensen MS, Mapendano CK *et al.* RNA exosome depletion reveals transcription upstream of active human promoters. *Science* 2008; **322**: 1851–1854.
15 Seila AC, Calabrese JM, Levine SS, Yeo GW, Rahl PB, Flynn RA *et al.* Divergent transcription from active promoters. *Science* 2008; **322**: 1849–1851.
16 Sigova AA, Mullen AC, Molinie B, Gupta S, Orlando DA, Guenther MG *et al.* Divergent transcription of long noncoding RNA/mRNA gene pairs in embryonic stem cells. *Proc Natl Acad Sci USA* 2013; **110**: 2876–2881.
17 Flynn RA, Almada AE, Zamudio JR, Sharp PA. Antisense RNA polymerase II divergent transcripts are P-TEFb dependent and substrates for the RNA exosome. *Proc Natl Acad Sci USA* 2011; **108**: 10460–10465.
18 Almada AE, Wu X, Kriz AJ, Burge CB, Sharp PA. Promoter directionality is controlled by U1 snRNP and polyadenylation signals. *Nature* 2013; **499**: 360–363.
19 Ntini E, Jarvelin AI, Bornholdt J, Chen Y, Boyd M, Jorgensen M *et al.* Polyadenylation site-induced decay of upstream transcripts enforces promoter directionality. *Nat Struct Mol Biol* 2013; **20**: 923–928.
20 Ozsolak F, Song JS, Liu XS, Fisher DE. High-throughput mapping of the chromatin structure of human promoters. *Nat Biotechnol* 2007; **25**: 244–248.
21 Wu X, Sharp PA. Divergent transcription: a driving force for new gene origination? *Cell* 2013; **155**: 990–996.
22 Rhee HS, Pugh BF. Genome-wide structure and organization of eukaryotic preinitiation complexes. *Nature* 2012; **483**: 295–301.
23 Marquardt S, Escalante-Chong R, Pho N, Wang J, Churchman LS, Springer M *et al.* A chromatin-based mechanism for limiting divergent noncoding transcription. *Cell* 2014; **157**: 1712–1723.
24 Andersson R, Gebhard C, Miguel-Escalada I, Hoof I, Bornholdt J, Boyd M *et al.* An atlas of active enhancers across human cell types and tissues. *Nature* 2014; **507**: 455–461.
25 Zhang L, Wang P, Ding Q, Wang Z. Transcriptional directionality of the human insulin-degrading enzyme promoter. *Mol Cell Biochem* 2013; **382**: 237–242.
26 Uesaka M, Nishimura O, Go Y, Nakashima K, Agata K, Imamura T. Bidirectional promoters are the major source of gene activation-associated non-coding RNAs in mammals. *BMC Genomics* 2014; **15**: 35.
27 Polson A, Reisman D. The bidirectional p53-Wrap53beta promoter is controlled by common cis- and trans-regulatory elements. *Gene* 2014; **538**: 138–149.
28 Hung T, Wang Y, Lin MF, Koegel AK, Kotake Y, Grant GD *et al.* Extensive and coordinated transcription of noncoding RNAs within cell-cycle promoters. *Nat Genet* 2011; **43**: 621–629.
29 Grote P, Wittler L, Hendrix D, Koch F, Wahrisch S, Beisaw A *et al.* The tissue-specific lncRNA Fendrr is an essential regulator of heart and body wall development in the mouse. *Dev Cell* 2013; **24**: 206–214.
30 Chao MP, Jaiswal S, Weissman-Tsukamoto R, Alizadeh AA, Gentles AJ, Volkmer J *et al.* Calreticulin is the dominant pro-phagocytic signal on multiple human cancers and is counterbalanced by CD47. *Sci Transl Med* 2010; **2**: 63ra94.
31 Chao MP, Majeti R, Weissman IL. Programmed cell removal: a new obstacle in the road to developing cancer. *Nat Rev Cancer* 2012; **12**: 58–67.
32 Obeid M, Tesniere A, Ghiringhelli F, Fimia GM, Apetoh L, Perfettini JL *et al.* Calreticulin exposure dictates the immunogenicity of cancer cell death. *Nat Med* 2007; **13**: 54–61.
33 Harrow J, Frankish A, Gonzalez JM, Tapanari E, Diekhans M, Kokocinski F *et al.* GENCODE: the reference human genome annotation for The ENCODE Project. *Genome Res* 2012; **22**: 1760–1774.
34 Adachi N, Lieber MR. Bidirectional gene organization: a common architectural feature of the human genome. *Cell* 2002; **109**: 807–809.
35 Manning AL, Dyson NJ. pRB a tumor suppressor with a stabilizing presence. *Trends Cell Biol* 2011; **21**: 433–441.
36 Hoesel B, Schmid JA. The complexity of NF-kappaB signaling in inflammation and cancer. *Mol Cancer* 2013; **12**: 86.
37 Luo J. Glycogen synthase kinase 3beta (GSK3beta) in tumorigenesis and cancer chemotherapy. *Cancer Lett* 2009; **273**: 194–200.
38 Fruman DA, Rommel C. PI3K and cancer: lessons, challenges and opportunities. *Nat Rev Drug Discov* 2014; **13**: 140–156.
39 Yang MQ, Koehly LM, Elnitski LL. Comprehensive annotation of bidirectional promoters identifies co-regulation among breast and ovarian cancer genes. *PLoS Comput Biol* 2007; **3**: e72.
40 Sakai T, Ohtani N, McGee TL, Robbins PD, Dryja TP. Oncogenic germ-line mutations in Sp1 and ATF sites in the human retinoblastoma gene. *Nature* 1991; **353**: 83–86.
41 Shiio Y, Yamamoto T, Yamaguchi N. Negative regulation of Rb expression by the p53 gene product. *Proc Natl Acad Sci USA* 1992; **89**: 5206–5210.
42 Shan B, Chang CY, Jones D, Lee WH. The transcription factor E2F-1 mediates the autoregulation of RB gene expression. *Mol Cell Biol* 1994; **14**: 299–309.
43 Savoysky E, Mizuno T, Sowa Y, Watanabe H, Sawada J, Nomura H *et al.* The retinoblastoma binding factor 1 (RBF-1) site in RB gene promoter binds preferentially E4TF1, a member of the Ets transcription factors family. *Oncogene* 1994; **9**: 1839–1846.
44 Gill RM, Hamel PA, Zhe J, Zacksenhaus E, Gallie BL, Phillips RA. Characterization of the human RB1 promoter and of elements involved in transcriptional regulation. *Cell Growth Differ* 1994; **5**: 467–474.
45 Sowa Y, Shiio Y, Fujita T, Matsumoto T, Okuyama Y, Kato D *et al.* Retinoblastoma binding factor 1 site in the core promoter region of the human RB gene is activated by hGABP/E4TF1. *Cancer Res* 1997; **57**: 3145–3148.
46 Hamel PA, Gill RM, Phillips RA, Gallie BL. Transcriptional repression of the E2-containing promoters EIIaE, c-myc, and RB1 by the product of the RB1 gene. *Mol Cell Biol* 1992; **12**: 3431–3438.
47 Lenhard B, Sandelin A, Carninci P. Metazoan promoters: emerging characteristics and insights into transcriptional regulation. *Nat Rev Genet* 2012; **13**: 233–245.
48 Gardai SJ, McPhillips KA, Frasch SC, Janssen WJ, Starefeldt A, Murphy-Ullrich JE *et al.* Cell-surface calreticulin initiates clearance of viable or apoptotic cells through trans-activation of LRP on the phagocyte. *Cell* 2005; **123**: 321–334.
49 Pandey RR, Mondal T, Mohammad F, Enroth S, Redrup L, Komorowski J *et al.* Kcnq1ot1 antisense noncoding RNA mediates lineage-specific transcriptional silencing through chromatin-level regulation. *Mol Cell* 2008; **32**: 232–246.
50 Carrieri C, Cimatti L, Biagioli M, Beugnet A, Zucchelli S, Fedele S *et al.* Long non-coding antisense RNA controls Uchl1 translation through an embedded SINEB2 repeat. *Nature* 2012; **491**: 454–457.
51 Wakano C, Byun JS, Di LJ, Gardner K. The dual lives of bidirectional promoters. *Biochim Biophys Acta* 2012; **1819**: 688–693.
52 Michalak M, Groenendyk J, Szabo E, Gold LI, Opas M. Calreticulin a multi-process calcium-buffering chaperone of the endoplasmic reticulum. *Biochem J* 2009; **417**: 651–666.
53 Siepel A, Bejerano G, Pedersen JS, Hinrichs AS, Hou M, Rosenbloom K *et al.* Evolutionarily conserved elements in vertebrate, insect, worm, and yeast genomes. *Genome Res* 2005; **15**: 1034–1050.
54 Langmead B, Trapnell C, Pop M, Salzberg SL. Ultrafast and memory-efficient alignment of short DNA sequences to the human genome. *Genome Biol* 2009; **10**: R25.
55 Trapnell C, Pachter L, Salzberg SL. TopHat: discovering splice junctions with RNA-Seq. *Bioinformatics* 2009; **25**: 1105–1111.
56 Trapnell C, Williams BA, Pertea G, Mortazavi A, Kwan G, van Baren MJ *et al.* Transcript assembly and quantification by RNA-Seq reveals unannotated transcripts and isoform switching during cell differentiation. *Nature Biotechnol* 2010; **28**: 511–515.
57 Bhatt DM, Pandya-Jones A, Tong AJ, Barozzi I, Lissner MM, Natoli G *et al.* Transcript dynamics of proinflammatory genes revealed by sequence analysis of subcellular RNA fractions. *Cell* 2012; **150**: 279–290.

Supplementary Information accompanies this paper on the Oncogene website (http://www.nature.com/onc)